52. Anion Cryptates: Synthesis, Crystal Structures, and Complexation Constants of Fluoride and Chloride Inclusion Complexes of Polyammonium Macrobicyclic Ligands

by **Bernard Dietrich, Brid Dilworth, Jean-Marie Lehn***, and **Jean-Paul Souchez**

Institut Le Bel, Université Louis Pasteur, 4, rue Blaise Pascal, F–67000 Strasbourg

and **Michèle Cesario, Jean Guilhem**, and **Claudine Pascard**

Laboratoire de Cristallochimie, Institut de Chimie des Substances Naturelles du CNRS, F–91190 Gif-sur-Yvette

Dedicated to the memory of *Willy Simon*

(27.XII.95)

Three macrobicyclic octamines **1–3** and the macrotricyclic hexadecamine **14** have been synthesized. The octamines **1–3** bind anionic substrates when protonated. The stability constants of the complexes between the protonated forms of the macrobicyclic polyamines and halide anions have been determined by pH-metric measurements. The stability constants in H_2O are very high; **1** in its hexaprotonated form binds F^- with high selectivity (selectivity $F^-/Cl^- > 10^8$), while **3** exhibits strong stability constants for both F^- and Cl^-. Three X-ray structures have been obtained, one where F^- is held inside the cavity of $\mathbf{1}\cdot 6H^+$, one where Cl^- is included in $\mathbf{3}\cdot 6H^+$, and $\mathbf{3}\cdot 6H^+$ where the cavity is empty.

Introduction. – In the last two decades, many synthetic molecules have been shown to form stable and selective complexes with various anions [1–12]. The design and synthesis of anion receptor and carrier molecules, leading to an anion-coordination chemistry, have developed markedly. In view of the role played by anionic species in chemical as well as in biological processes, their binding by synthetic receptor molecules is of wide interest.

Among the classes of anion ligands and complexes that have been reported, particularly stable and selective are the anion inclusion complexes, the katapinates [13] and anion cryptates [14–22], in which the anionic substrate is bound inside the intramolecular cavity of a macrocyclic or macropolycyclic molecule. The anion-complexation units of these receptor molecules consist of several positively charged binding sites arranged around a cavity defined by the macropolycyclic architecture.

The stability constants of the complexes formed between the protonated forms of the macrobicyclic ligand 'bis-tren' **A** and various anions have been determined [19]. For the halide ions, the stability constants in H_2O are significant although not very high (log $K_s = 4.40$ for F^-, 3.00 for Cl^-, and 2.60 for Br^-), and this ligand exhibits only a moderate selectivity in favor of F^-. Improved selectivity has been observed with a macrotricyclic ligand **B** [14], the selectivity ratio Cl^-/Br^- being greater than 10^3. Ligands presenting a high selectivity for each of the halide ions would be of much interest for both basic and applied reasons. We present here our results on macrobicyclic receptor molecules for F^- and Cl^- ions.

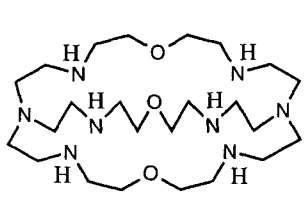

A 'bis-tren'

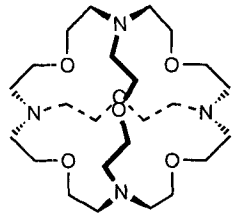

B

Design of the Polyaza Receptor Molecules. – To achieve high selectivity in favor of F^-, a ligand displaying a small cavity of size complementary to F^- (ionic radius = 1.33 Å) has to be synthesized. As revealed by the X-ray structure [19], the 'bis-tren' ligand **A** is too large for F^-. Consideration of the cavity size of cation cryptates [23] indicated that the peraza analogue **1** should present the required geometric features: a cavity of spheroidal shape, of suitable size, and lined with six secondary ammonium sites in the hexaprotonated state. This cryptand has been synthesized by a stepwise method [22]. An efficient multicondensation approach, involving a double tripode coupling, has also been described recently [24].

To determine the effect of structural variations on binding strength and selectivity, the permethylated derivative **2** as well as the extended macrobicycle **3** possessing an enlarged cavity were synthesized as well. The latter could display an interesting shift towards selectivity for the Cl^- ion. In addition, the unprotonated polyamines **1–3** are expected to bind efficiently transition- and heavy-metal ions in a given geometric arrangement [25] [26].

Synthesis of the Macrobicycles 1–3. – The macrobicycle **1** was obtained either by the stepwise route shown in *Scheme 1,a*, or by the multiple condensation method (*Scheme 1,b*) [24]. The latter provides direct access to the final compound. The former is more flexible and makes available intermediate substances of interest for the synthesis of other structures. Ditosylethylenediamine **4** was alkylated with chloroacetonitrile in DMF in the presence of K_2CO_3 to yield the dicyano compound **5**, which was reduced to the diamine **6** by treatment with diborane in THF. The latter was then condensed with the diacyl dichloride **7** under high-dilution conditions, yielding the macrocyclic derivative **8** (38% yield; see *Footnote a* in *Scheme 1*), which was further reduced to **9** with diborane in THF and condensed again with one molecule of **7** under high-dilution conditions affording the macrobicycle **10** in 28% yield as well as the macrotricyclic dimer **12** (see below, *Scheme 2*) in 9% yield. Several examples of competitive [2+2] cyclocondensations have been described [28–31]. The main factors contributing to the formation of a macrotricyclic system are (depending on the case): *i*) the small sizes of the monocycle and of the incoming chain (difficulty of formation of medium rings), *ii*) the rigidity of the incoming chain, and *iii*) steric hindrance. The last two factors are certainly to be considered in our case. Only the stepwise synthesis allowed the isolation of the dimer. The bis-lactam **10** obtained was then reduced with diborane in THF to give **11** and the tosyl groups removed yielding the target ligand **1**. The permethylated derivative **2** was obtained by applying the *Eschweiler-Clarke* procedure to the parent compound **1**.

Scheme 1. *Synthesis of the Macrobicyclic Polyamines* **1** *and* **2**[a])

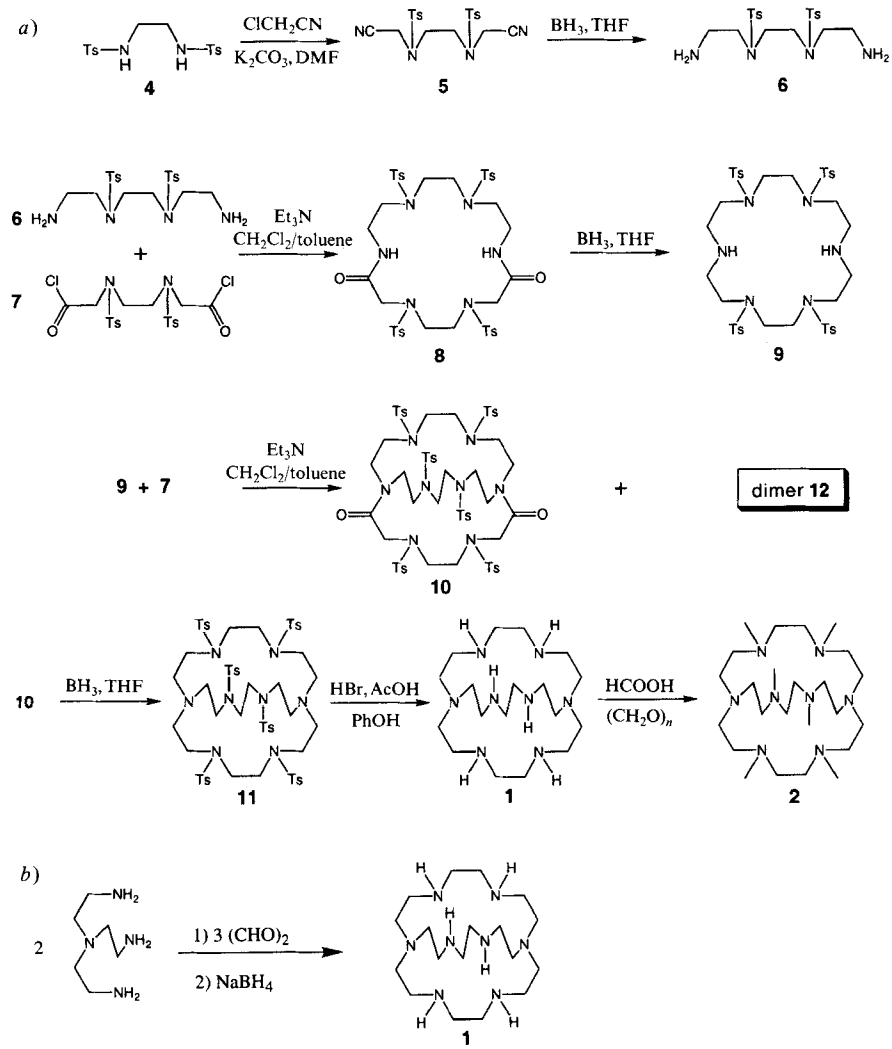

[a]) The synthesis of macrocycle **8** was already described: the same cyclization method was used, but the preparation of diamine **6** was different [27].

The dimer **12** was also reduced to yield **13**, and this compound was detosylated to afford the macrotricyclic polyamine **14**.

The macrobicycle **3** was synthesized by the coupling of two tripodes (*Scheme 3*). The tritosylamide **15** was alkylated in acetonitrile by methyl acrylate in the presence of K_2CO_3, yielding the triester **16**, which was further reduced to the trialcohol **17** with $LiAlH_4$ in THF. Mesylation of **17** afforded **18** which was condensed with **15** to yield the macrobicycle **19** in 31% yield. Removal of the tosyl groups gave the target ligand **3**.

Scheme 2. *Synthesis of the Macrotricyclic Polyamine* **14**

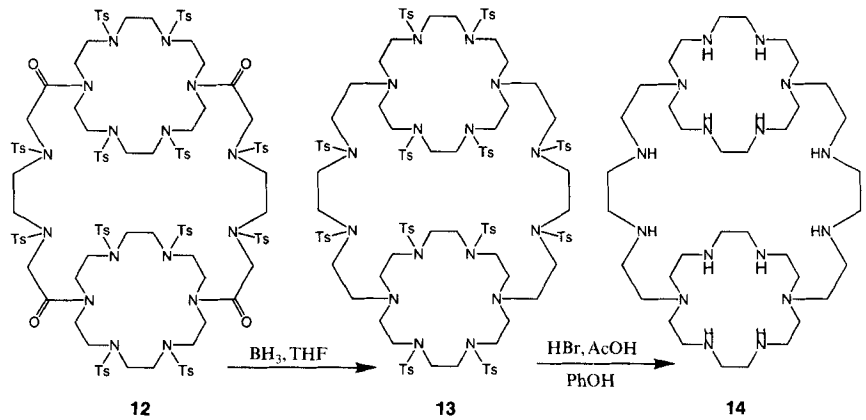

Scheme 3. *Synthesis of the Macrobicyclic Polyamine* **3**

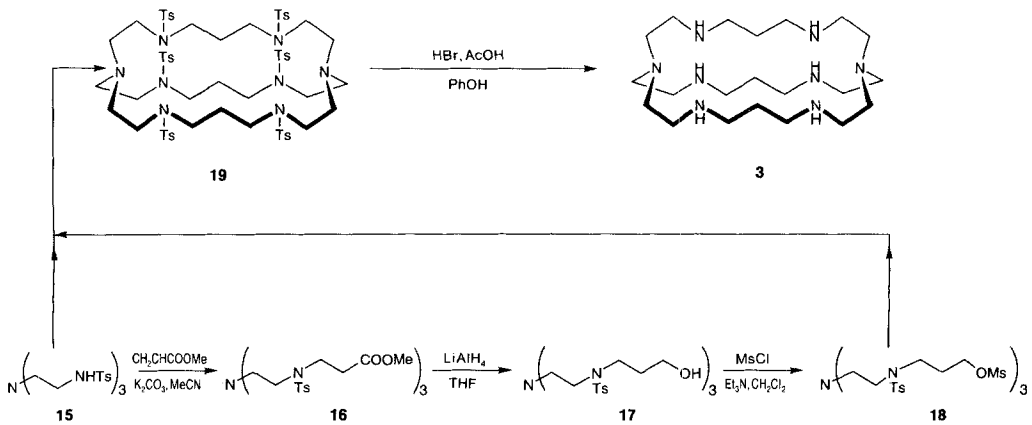

Stability Constants for Anion Binding by Ligands $1 \cdot n\mathrm{H}^+$, $2 \cdot n\mathrm{H}^+$, and $3 \cdot n\mathrm{H}^+$. – *Protonation Features of the Macrobicycles* **1–3**. pH-Metric titrations of the polyamines **1–3** gave the acidity constants log K_n ($= \mathrm{p}K_a$ values) corresponding to the protonation equilibria of the polyamines **1–3** (*Eqns. 1* and *2*), which are listed in *Table 1*. For ligand **1**, a cumulated value has been obtained for the last two protonations, corresponding to a two-proton uptake (see also [32] [33]).

$$\mathrm{H}_{n-1}\mathrm{L}^{(n-1)+} + \mathrm{H}^+ \rightleftharpoons \mathrm{H}_n\mathrm{L}^{n+} \tag{1}$$

$$\mathrm{K}_n = \frac{[\mathrm{H}_n\mathrm{L}^{n+}]}{[\mathrm{H}_{n-1}\mathrm{L}^{(n-1)+}][\mathrm{H}^+]} \tag{2}$$

It is seen that the $\mathrm{p}K_a$'s corresponding to the last protonations are very low, especially in the case of **1**, as the protonation sites lie in close proximity. One can notice that our

Table 1. *Acidity Constants* pK_a ($\log K_n$) *of the Macrobicyclic Polyamines* **1–3**

n	**1**[a])	**1**[b])	**2**[a])	**3**[a])
1	10.70	11.18	10.05	9.85
2	9.20	9.43	9.70	9.35
3	7.50	7.59	8.20	8.00
4	5.50	5.78	5.75	6.85
5			3.40	5.75
6	5.10[c])	4.39[c])	2.30	4.40

[a]) 0.1M $(Me_4N)TsO$, 25°. [b]) 0.1M KNO_3, 25° [32]. [c]) $pK_5 + pK_6$ cumulated value.

results are in good agreement with the pK_a's measured in a different supporting electrolyte (0.1M KNO_3 [32]).

Anion Complexation Features of the Protonated Ligands **1–3**. The stability constants $\log K_s^n$ corresponding to the equilibria of the polyammonium ions H_nL^{n+} (L = **1–3**) with the anions A^- (A = F, Cl, Br, I; *Eqns. 3* and *4*) have been determined by computer analysis of the pH-metric titration curves measured in presence of the corresponding anion. The results are listed in *Table 2*.

$$L + nH^+ + A^{m-} \rightleftharpoons (H_nLA)^{(n-m)+} \tag{3}$$

$$K_s^n = \frac{[(H_nLA)^{(n-m)+}]}{[H^+]^n[L][A^{m-}]} \tag{4}$$

Table 2. *Stability Constants* $\log K_s^n$ *for the Complexation of Halide Ions by the Protonated Macrobicyclic Polyamines* $\mathbf{1}\cdot nH^+$, $\mathbf{2}\cdot nH^+$, *and* $\mathbf{3}\cdot nH^+$

	n	F^-[a])	Cl^-	Br^-	I^-
1	6	10.55[b])	< 2	–	–
	5	8.40[b])	–	–	–
	4	5.20[b])	–	–	–
	3	3.30[b])	–	–	–
2	6	7.85	1.70	–	–
	5	6.30	–	–	–
	4	4.55	–	–	–
3	6	6.10	5.75	4.40	2.25
	5	4.35	3.75	2.40	2.00
	4	2.75	2.40	1.95	1.70

[a]) The equilibrium constant ($\log K = 3.25$) for HF ($K = [HF]/[H^+][F^-]$) was included in the calculations.
[b]) The stability constants obtained by *Smith* and coworkers [32] in another supporting electrolyte are 11.2, ≥ 8.8, 5.1, and 3.6, respectively.

In agreement with the structural data (*vide infra*), 1:1 substrate/ligand stoichiometries were assumed in all cases. To minimize interference from other anions, $(Me_4N)TsO$ was used as supporting electrolyte.

It is seen that compound $\mathbf{1}\cdot 6H^+$ exhibits a very strong F^-/Cl^- selectivity (> 10^8), and that the stability constants are very high compared to the ligands investigated previously

[19], indicating a much better complementarity between F^- and the ligand, in agreement also with the X-ray structure showed. Similar results were obtained in an independent work [32]. Moreover, $\mathbf{2}\cdot 6H^+$ presents also a high F^-/Cl^- selectivity; the stability constant for F^- is, nevertheless, somewhat smaller than for $\mathbf{1}\cdot 6H^+$, since only one H-atom is now available on each N-atom for interacting with F^-.

The extended macrobicycle $\mathbf{3}\cdot 6H^+$ displays high stability constants for both F^- and Cl^-, and appreciable selectivity is found for Cl^-/Br^- and Cl^-/I^-. This corresponds to the good match between the cavity present in **3** and the ionic radius of Cl^- (1.81 Å).

Structural Results. – Structural data for anion complexation are still limited to few examples, compared to the vast amount of information on cation complexes. There is, therefore, a need to obtain further structural information on this type of complexes.

We report here two crystal structures of anion cryptates $[F^- \subset \mathbf{1}\cdot 6H^+]$ and $[Cl^- \subset \mathbf{3}\cdot 6H^+]$. We describe also the structure of the ligand $\mathbf{3}\cdot 6H^+$ with an empty cavity, obtained by using the bulky tosylate as counter-anion. In view of the very large number of bond lengths and bond angles present in the three structures studied here, only selected values directly relevant to the discussion of these three systems are given (see below, *Tables 4–6*), *i.e.*, those concerning the coordination geometry around the anions (internal and external binding) and the geometry of the ligands. The experimental procedures for data collection and refinement, and the crystal-structure data are summarized in *Table 3*. All other results are contained in supplementary material obtainable on request from the *Cambridge Crystallographic Data Centre*, 12 Union Road, Cambridge CB2, 1EZ, England.

Table 3. *Crystal-Structure Data*

	$[F^- \subset \mathbf{1}\cdot 6H^+]$	$[\mathbf{3}\cdot 6H^+]$	$[Cl^- \subset \mathbf{3}\cdot 6H^+]$
Formula	$[C_{18}H_{48}N_8F]\cdot F_2Cl\cdot 2PF_6\cdot 5H_2O$	$[C_{21}H_{54}N_8]\cdot 6C_7H_7SO_3\cdot 6.5H_2O$	$[C_{21}H_{54}N_8Cl]\cdot Cl_5\cdot 3.5H_2O$
Molecular weight	794.5	1561	685
Crystal system	triclinic	triclinic	monoclinic
Space group	$P\bar{1}$	$P\bar{1}$	$P2_1/n$
a [Å]	17.199(12)	16.258(7)	18.797(9)
b [Å]	11.385(6)	17.396(8)	15.596(8)
c [Å]	10.395(6)	18.309(9)	12.697(6)
α [°]	106.66(5)	94.65(5)	90.0
β [°]	81.74(5)	116.97(9)	106.37(5)
γ [°]	107.10(5)	113.84(8)	90.0
V [Å^3]	1860	3993	3571
Z	2	2	4
d(calc)	1.51	1.30	1.29
F(000)	1486	1563	1328
λ	CuK_α	MoK_α	CuK_α
μ [mm^{-1}]	44	0.23	44
Range measured	2–68°	5–28°	2–68°
Scan type	$\theta/2\theta$	$\theta/2\theta$	$\theta/2\theta$
Reflections measured	7328	12252	6468
Reflections used $I > 3\sigma(I)$	2525	4709	3186
No. of parameters	203	213	346
Final R (unweighted)	8.9%	7.5%	7.0%

Fluoride Cryptate. $[F^- \subset \mathbf{1} \cdot 6H^+] \cdot 2F^- \cdot Cl^- \cdot 2PF_6^-$. A short preliminary report of this structure has been described in a previous publication [22]. *Fig. 1* shows the ligand with the inner F^- ion H-bonded to the six protonated N-atoms of the macrobicycle and the ternary symmetry of the complex.

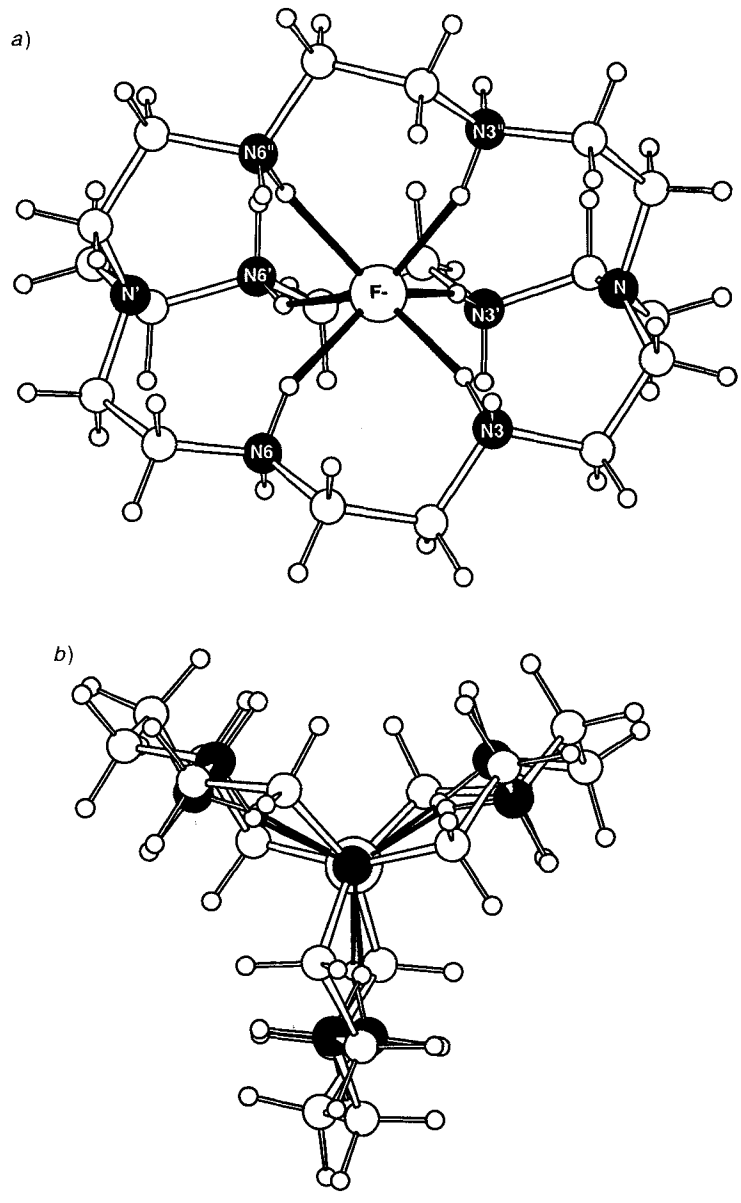

Fig. 1. *Crystal structure of the fluoride cryptate* $[F^- \subset \mathbf{1} \cdot 6H^+]$: a) *ORTEP representation perpendicular to* $N-N'$ *axis and* b) *view down the ternary axis* $N-N'$

The F^-–N^+ distances range from 2.76 to 2.88 Å, and the distances of F^- to the bridgehead N-atoms (N,N′) are slightly different: 3.28 and 3.37 Å (*Table 4*). This may result from the heterogeneous character of the ligand environment and by its strong binding to the external F^- and Cl^- counterions; indeed, the distances between the protonated N-atoms, and the internal and external F^- ions are of the same order (*Table 4*).

Table 4. *Structural Data* (distances in Å) *for the Fluoride Cryptate* [$F^- \subset \mathbf{1}\cdot 6H^+$][a])

Distances of the N-atoms and H-atoms at N^+ to the inner F^- (F(1); σ(N–F) = 0.01 Å)							
N–N′	6.65						
N(3)–F(1)	2.82	H(31)–F(1)	1.85	N(6)–F(1)	2.86	H(61)–F(1)	1.93
N(3′)–F(1)	2.76	H(3′1)–F(1)	1.80	N(6′)–F(1)	2.88	H(6′1)–F(1)	1.99
N(3″)–F(1)	2.84	H(3″1)–F(1)	1.88	N(6″)–F(1)	2.86	H(6″1)–F(1)	1.96
N–F(1)	3.28			N′–F(1)	3.37		
External binding of the protonated N-atoms (N^+)							
N(3)–F(3)	2.86	H(32)–F(3)	1.96	N(6)–F(2)	2.78	H(62)–F(2)	1.82
N(3′)–Cl(1)	3.12	H(3′2)–Cl(1)	2.13				
N(3″)–W(2)	2.71[b])	H(3″2)–W(2)	1.73	N(6″)–F2X[c])	2.85	H(6″2)–(PF_6)	1.87
External counter-anions and H_2O binding (H-bonds)							
Cl(1)–F(2)	3.11			W(1)–W(2)	2.71		
Cl(1)–W(4)	3.27			W(1)–W(3)	2.83		
F(3)–W(5)	3.06			W(3)–W(5)	3.07		
F(3)–W(5′)	2.85			W(4)–W(5)	2.72		

[a]) Arbitrary numbering. [b]) W = O-Atom of H_2O molecules. [c]) F2X is one of the stable F of an external disordered PF_6^-.

Ligand $\mathbf{1}\cdot 6H^+$ has nearly perfect dimensions to form a cryptate inclusion complex with the F^- ion.

Uncomplexed Ligand $\mathbf{3}\cdot 6H^+\cdot 6TsO^-$. *Fig. 2* represents the solid-state structure of the uncomplexed ligand $\mathbf{3}\cdot 6H^+$. The corresponding dimensions are listed in *Table 5*.

The macrobicycle has a non-crystallographic binary symmetry, with a single diad axis passing through the central atom of one lobe and perpendicular to the N–N′ axis. Consequently, one lobe is symmetrical, and the other two, related by the diad axis, are dissymmetrical. Two faces are equivalent, the third one is much larger. This correlates with the directions of the lone pairs at N and N′ which are not aligned and make an angle of 60° with the N–N′ axis. They are directed through the symmetrical faces, towards two counterions: tosylates t1 and t2.

All the protonated N-atoms are linked externally through their H-atoms to tosylate O-atoms and H_2O molecules. Three tosylates t1, t2, and t4 are situated between the 3 bridges and link the two flanking lobes through H-bonds.

Chloride Cryptate [$Cl^- \subset \mathbf{3}\cdot 6H^+$]$\cdot 5Cl^-$. *Fig. 3* represents the chloride cryptate; selected structural data are listed in *Table 6* and compared with those of [$Cl^- \subset$ 'bistren'$\cdot 6H^+$]. Whereas, in the larger macrobicycle, the N–N′ axis is not a ternary axis of symmetry but a diad axis passing through the central chloride, the cryptate [$Cl^- \subset \mathbf{3}\cdot 6H^+$] has a quasi-perfect ternary symmetry around the bridgehead N–N′ axis clearly visible in *Fig. 3, b*.

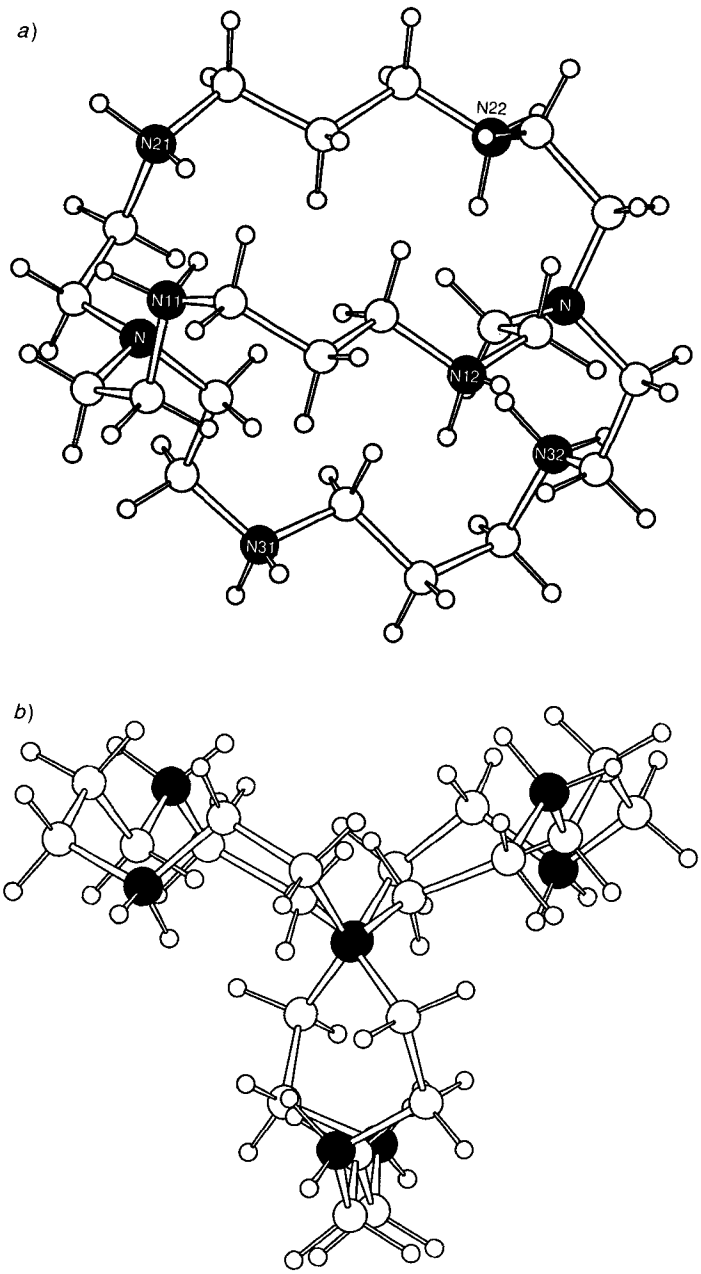

Fig. 2. *Crystal structure of the uncomplexed ligand* $\mathbf{3}\cdot 6H^+$: a) *view perpendicular to* $N-N'$ *axis and* b) *view down the* $N-N'$ *axis*

Table 5. *Structural Data* (distances in Å, angles in °) *for the Uncomplexed Ligand* $3 \cdot 6H^{+}$[a])

Dimensions of the cavity (σ = 0.015 Å, 1°)					
N–N′	6.08	N–N(11)	2.96(1)	N′–N(12)	2.92
C(14)–C(24)	6.46	N–N(21)	3.83(1)	N′–N(22)	2.99
C(14)–C(34)	6.42	N–N(31)	2.99(1)	N′–N(32)	3.80
C(24)–C(34)	7.44	N(11)–N(21)	5.88	N(12)–N(22)	4.61
		N(11)–N(31)	4.59	N(12)–N(32)	5.87
		N(21)–N(31)	6.02	N(22)–N(32)	5.79
N–O(1t2)	3.48	N′–O(3t1)	3.55		
d–O(1t2)[a])	2.88	d′–O(3t1)[a])	3.20	d–N–N′–d′	−120°
S(2)–O(1)–N:	126°	S(1)–O(3)–N′	120°		

External binding of the protonated N-atoms (H-bonds)[b])			
N(11)–O(1t2(*i*))	2.90	H(111)–O(1t2(*i*))	1.98
N(11)–O(3t2(*ii*))	2.77	H(211)–O(3t2(*ii*))	1.81
N(12)–O(2t1(*i*))	2.75	H(112)–O(2t1(*i*))	1.79
N(12)–O(1t1(*iii*))	2.98	H(212)–O(1t1(*iii*))	2.09
N(21)–O(2t6(*i*))	2.65	H(121)–O(2t6(*i*))	1.70
N(21)–O(1t4(*i*))	2.70	H(221)–O(1t4(*i*))	1.71
N(22)–O(1t1(*iii*))	3.06	H(122)–O(1t1(*iii*))	2.10
N(22)–O(3t1(*i*))	2.93	H(222)–O(3t1(*i*))	2.24
N(22)–O(3t5(*i*))	2.99	H(222)–O(3t5(*i*))	2.28
N(31)–O(1t2(*i*))	2.98	H(231)–O(1t2(*i*))	2.02
N(31)–O(W2(*i*))	2.83	H(131)–O(W2(*i*))	2.01
N(32)–O(3t4(*i*))	2.90	H(132)–O(3t4(*i*))	1.93
N(32)–O(W1(*i*))	2.77	H(232)–O(W1(*i*))	1.77

[a]) Arbitrary numbering. d and d′: lone pairs on N and N′; t*n* (*n* = 1, 6): tosylate counterions.

[b]) Symmetry code: *i* = *x*,*y*,*z*; *ii* = −*x*,−*y*,−*z*; *iii* = 1−*x*,−*y*,1−*z*.

It is noteworthy that the 6.08-Å distance between the bridgehead N-atoms of the free ligand $3 \cdot 6H^{+}$ elongates to as much as 7.60 Å when it encapsulates Cl^{-} (cryptate [$Cl^{-} \subset$ 'bis-tren' $\cdot 6H^{+}$]: 7.40 Å). As in the [$Cl^{-} \subset$ 'bis-tren' $\cdot 6H^{+}$] cryptate, the included Cl^{-} ion is situated on the N–N′ axis. But, whereas in the first structure, Cl^{-} is located on the diad axis and, therefore, in the middle of N–N′, in the present structure [$Cl^{-} \subset 3 \cdot 6H^{+}$], it is closer to one cap of the macrobicycle than to the other: Cl^{-}–N 3.905 and Cl^{-}–N′ 3.700 Å. This is due to the larger Cl^{-}–N^{+} distances (average 3.32 Å) on one side than on the other (3.16 Å) (see *Table 6*). Accordingly, in the N′ cap to which Cl^{-} is closer, the H-bonds between the protonated N-atoms and the included anion are more aligned (Cl^{-}–H–N^{+} angle of 150° average) than for the N cap (123° average).

Ligand Environment of the Chloride Cryptate [$Cl^{-} \subset 3 \cdot 6H^{+}$*] ·* $5Cl^{-}$*: Formation of a Clathrate.* The environment of the ligand plays a key role in the molecular dissymmetry of each lobe of the macrobicycle (*Table 6*).

Fig. 4, a, shows the cryptate surrounded by external Cl^{-} ions which obey the same ternary symmetry. These anions are situated at the level of the protonated N-atoms of the N cap from which the internal Cl^{-} ion is farther. They are inserted in the space between each lobe, and each one, in turn, is bound to a H_2O molecule. Each Cl^{-} ion located outside

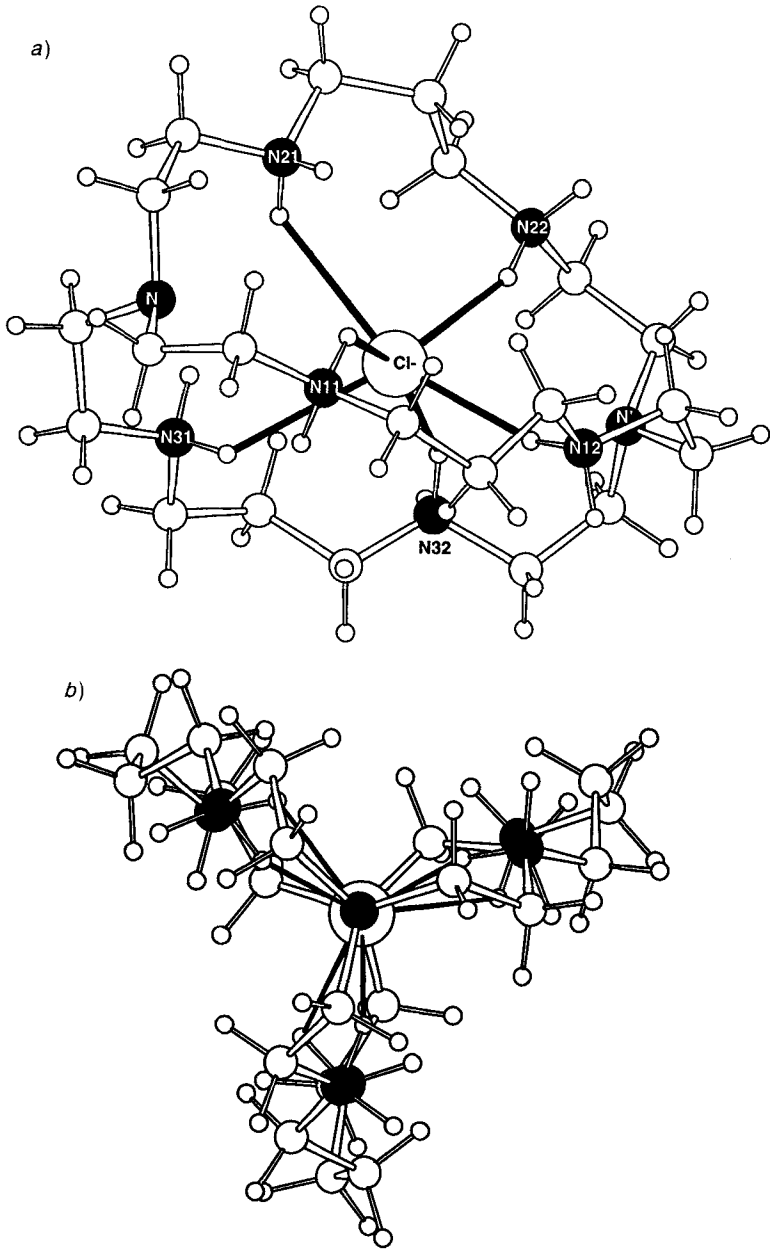

Fig. 3. *Crystal structure of the chloride cryptate* $[Cl^- \subset \mathbf{3} \cdot 6H^+]$*:* a) *ORTEP representation view perpendicular to the* $N-N'$ *axis and* b) *view down the ternary* $N-N'$ *axis*

Table 6. *Structural Data* (distances in Å, angles in °) *for the Chloride Cryptate* $[Cl^- \subset \mathbf{3}\cdot 6H^+]$ *and for the Related* $[Cl^- \subset$ *'bis-tren'* $\cdot 6H^+]$[a])

Dimensions of the cavity (σ(N–N) 0.01 Å, σ(Cl–N) 0.007 Å for $[Cl^- \subset \mathbf{3}\cdot 6H^+]$)					
$[Cl^- \subset$ 'bis-tren' $\cdot 6H^+]$		$[Cl^- \subset \mathbf{3}\cdot 6H^+]$			
N–N′	7.40	N–N′	7.60		
O(1)–O(2)[b])	5.28	C(14)–C(24)[b])	6.46		
O(1)–O(3)[b])	6.14	C(14)–C(34)[b])	6.47		
O(2)–O(3)[b])	6.14	C(24)–C(34)[b])	6.61		
		N–N(11)	2.84	N(11)–N(21)	4.32
		N–N(21)	3.02	N(11)–N(31)	4.15
		N–N(31)	2.99	N(21)–N(31)	4.27
		N′–N(12)	3.01	N(12)–N(22)	4.33
		N′–N(22)	3.06	N(12)–N(32)	4.28
		N′–N(32)	3.03	N(22)–N(32)	4.29
$N–N^+$	3.11 (average)				
$N^+–N^+$	4.25, 4.32, and 4.80				

Internal Cl^- (Cl(1)) binding in $[Cl^- \subset \mathbf{3}\cdot 6H^+]$ (σ(Cl–N) = 0.007 Å, σ(Cl–W) = 0.008 Å, angle (σ = 0.6°))[c])					
	Cl(1)–N	3.905		Cl(1)–C(14)	3.783
	Cl(1)–N′	3.700		Cl(1)–C(24	3.825
				Cl(1)–C(34)	3.683
N(11)–Cl(1)	3.380	H(211)–Cl(1)	2.72	N(11)–H–Cl(1)	124.4
N(21)–Cl(1)	3.306	H(221)–Cl(1)	2.63	N(21)–H–Cl(1)	124.8
N(31)–Cl(1)	3.290	H(131)–Cl(1)	2.68	N(31)–H–Cl(1)	119.5
N(12)–Cl(1)	3.147	H(212)–Cl(1)	2.25	N(12)–H–Cl(1)	148.4
N(22)–Cl(1)	3.154	H(222)–Cl(1)	2.23	N(22)–H–Cl(1)	154.4
N(32)–Cl(1)	3.169	H(232)–Cl(1)	2.26	N(32)–H–Cl(1)	149.5

Binding of protonated N-atoms to external Cl^- ions[d])					
N(11)–Cl(2)	3.134	H(111)–Cl(2)	2.15	N(11)–H–Cl(2)	168.2
N(11)–Cl(5)	3.312	H(211)–Cl(5)	2.50	N(11)–H–Cl(5)	137.6
N(21)–Cl(5)	3.121	H(121)–Cl(5)	2.13	N(21)–H–Cl(5)	169.9
N(21)–Cl(3)	3.221	H(221)–Cl(3)	2.45	N(21)–H–Cl(3)	133.7
N(31)–Cl(3)	3.201	H(231)–Cl(3)	2.22	N(31)–H–Cl(3)	165.6
N(31)–Cl(2)	3.252	H(131)–Cl(2)	2.45	N(31)–H–Cl(2)	137.4
N(12*jj*)–Cl(4*j*)	3.082	H(112*jj*)–Cl(4*j*)	2.09	N(12*jj*)–H–Cl(4*j*)	169.3
N(22*j*)–Cl(4*j*)	3.101	H(122*jj*)–Cl(4*j*)	2.10	N(22*j*)–H–Cl(4*j*)	175.2
N(32*j*)–Cl(6*j*)	3.085	H(132*j*)–Cl(6*j*)	2.09	N(32*j*)–H–Cl(6*j*)	173.1
	W(1*jjj*)–Cl(6*j*)	3.178		W(2)–Cl(3) 3.216	
	W(1*jjj*)–Cl(5*jjj*)	3.091		W(3)–Cl(2) 3.225	

[a]) Arbitrary numbering.
[b]) Central atom of the lobes.
[c]) In $[Cl^- \subset$ 'bis-tren' $\cdot 6H^+]$: Cl(1)–N 3.71 and Cl(1)–O 3.25 Å.
[d]) Symmetry code: $j = x,y,z$; $jj = 2.5-x,0.5+y,0.5-z$; $jjj = x,y,-1+z$.

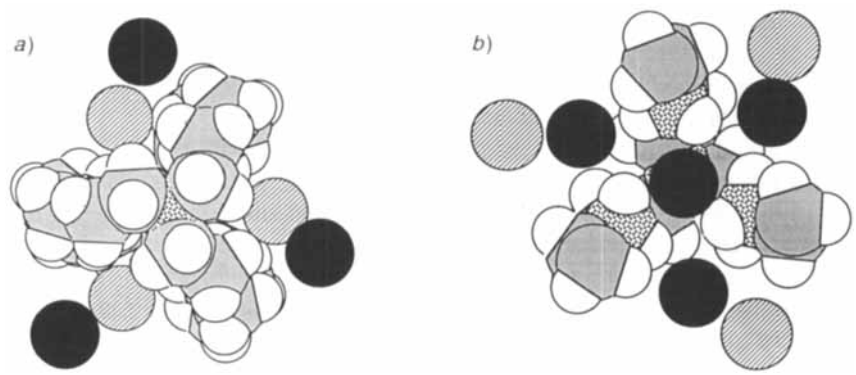

Fig. 4. *Chloride cryptate [$Cl^- \subset 3 \cdot 6H^+$]:* a) *CPK representation of the molecule down the N–N′ axis* (dotted atom: bridgehead N′) *and* b) *cryptate cut in half showing the sequestered Cl^- ion bonded to 3 NH^+ groups and 3 external Cl^- ions bonded to a H_2O molecule and also bonded to the same NH^+ groups.* Black spheres: Cl^-, streaked spheres: H_2O molecules, dotted spheres: N.

the ligand links the two flanking lobes; it forms on one side a direct H-bond to one protonated N-atom N(i1)$^+$ (average distance 3.15 Å; Cl(i)$^-$–H average distance 2.16 Å) and, on the other side, shares a binding H-atom (bifurcated H-bond) with the internal Cl^- ion (average distance 3.26 Å; Cl(i)–H average distance 2.47 Å). The triangle formed by these anions is slightly rotated around the N–N′ axis with respect to the lobes, so that the anions are not equidistant from the protonated N(i1)$^+$.

Fig. 4, b, which is obtained by cutting the ligand in two parts perpendicularly to the N–N′ axis, illustrates clearly the relative positions of the internal Cl^- and the three external Cl^- ions. The protonated N-atoms N(i2)$^+$ of the N′ cap are also bound to external anions, but in a different way:

An isolated Cl^- ion, Cl(4)$^-$ is sequestered between two molecules related by the 2_1 screw axis (*Fig. 5*). It binds strongly to the two ligands through two short H-bonds (mean values: 3.10 Å and 173° for the H-binding angle), thus forming a

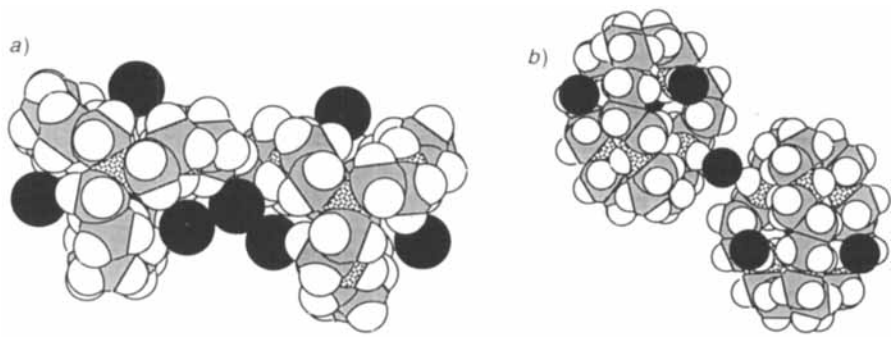

Fig. 5. *Chloride cryptate [$Cl^- \subset 3 \cdot 6H^+$]; two ligands related by the crystallographic screw axis enclosing Cl(4) anion:* a) *view down the N–N′ axes of the two nearly parallel molecules* (dihedral angle of 6°) *and* b) *perpendicular view to the N–N′ axes.* Dotted spheres = N.

clathrate type of structure. The molecules are connected *via* intermolecular $^{+}N(12)-H\cdots Cl(4)^{-}\cdots H-N(22)^{+}$ bonds along the *b* axis. Along the *c* direction, the molecules are linked by H-bonds through a H_2O molecule: $^{+}N(32)H\cdots Cl(6)\cdots W(1)\cdots Cl(5)\cdots HN(21)^{+}$.

A very good consistency can be observed among H-bond lengths and angles, the shorter bonds being associated as usual with the larger angles. The ternary symmetry gives all values by triads. Considering both the internal and external $Cl^{-}-N^{+}$ distances, the shortest ones link the external anions with almost linear H-bonds (angle $^{-}Cl-H-N^{+}$ *ca.* 170°). Consequently, it appears that macrocycle **3**·6H^{+} is still somewhat too large for a tight encapsulation of the Cl^{-} ion. In addition, the anionic environment plays an important role in distorting the ligand, thus displacing slightly the internal Cl^{-} off-center. The external Cl^{-} ions are small enough to insert between the lobes. Larger counter-anions would be expected to interfere less so that the cryptated anion could be more centered.

Discussion. – The ligands **1**·6H^{+} and **2**·6H^{+} present both very strong anion-binding properties and very high F^{-}/Cl^{-} selectivities (> 10^{8} and 10^{6}, resp.). On the contrary, the ligand **3**·6H^{+} does not exhibit Cl^{-}/F^{-} selectivity. To gain a better understanding of these results, it is of interest to compare the behavior of the anion-complexing ligands to that of the cation-complexing cryptands.

The ligands **1**·6H^{+} and **2**·6H^{+} display both a very sharp *peak selectivity* for F^{-}, as do the small cryptands [2.1.1], [2.2.1], and [2.2.2] for Li^{+}, Na^{+}, and K^{+}, respectively [34]. The ligand **3**·6H^{+} which is slightly larger than **1** presents a markedly increased chloride binding but no Cl^{-}/F^{-} selectivity. The above mentioned cryptands are able to discriminate against cations which are either smaller or larger than their cavity, since distortion of the ligand either by contraction or by expansion of its cavity leads to steric strain in the ligand backbone and, therefore, to pronounced destabilization of the complex. The ligands **1**·6H^{+} and **2**·6H^{+} have the same behavior as cryptand [2.1.1], *i.e.*, high selectivity for the smallest ions (F^{-} and Li^{+}, resp.). Unlike cryptand [2.2.1], which presents selectivity for Na^{+} against smaller (Li^{+}) or larger (K^{+}) cations, the ligand **3**·6H^{+} presents only selectivity against larger anions (Br^{-} and I^{-}). Two factors can explain the behavior of **3**·6H^{+}. Firstly, as seen in the structural part, the ligand is apparently slightly too large for Cl^{-}, but this explanation has a major drawback, since a smaller ligand would complex even better the F^{-} ion, and, therefore, a significant Cl^{-}/F^{-} selectivity improvement would not be observed. Secondly, the contraction of the ligand **3**·6H^{+} to adapt its cavity to the size of the smaller F^{-} anion does not bring the expected destabilization of the complex (as observed with [2.2.1] for Li^{+}).

The main reason may be the very strong H-bonds formed with F^{-}. This dominant factor is supported by the large variety of coordination numbers and geometries encountered in published structures of F^{-} complexes: *i*) in the [F ⊂ 'bis-tren'·6H^{+}] complex, the anion is tetracoordinated and the F^{-} anion has a tetrahedral coordination geometry; the strength of the H-bonds is illustrated by the fact that the ligand is strongly distorted [19]; *ii*) in the above described [F^{-} ⊂ **1**·6H^{+}] complex, the anion is hexacoordinated in a quasi-trigonal prismatic geometry; *iii*) in the F^{-} complex formed with deprotonated sapphyrin, the anion is pentacoordinated and lies within the plane formed by the five N–H coordination sites [35–37]; this ligand displays a F^{-}/Cl^{-} (or F^{-}/Br^{-}) selectivity higher than 10^{3} in MeOH [36].

These three examples indicate that the F^- anion accomodates itself to various coordination geometries, provided it can form strong H-bonds. The versatility of F^- binding constitutes a major handicap for the design of a Cl^--selective ligand.

Conclusion. – The present results provide insight into the structural features of anion-coordination complexes and allow an analysis of the binding properties in terms of receptor-substrate complementarity.

The data indicate that hexaprotonated **1** binds F^- very strongly and very selectively in aqueous solution, and $\mathbf{3}\cdot 6H^+$ binds strongly both F^- and Cl^-.

Since alkylation of the N-atoms yields ligands retaining high binding stability, it should be possible to synthesize derivatives of these anion cryptands using the N-atoms as a handle for anchoring other groups. It would then be possible to combine the selective binding properties of the ligands with photochemically or electrochemically active units leading to polyfunctional supramolecular devices. More specifically, **1**, fitted with light absorbing/emitting groups, could yield a highly sensitive and selective optical probe for fluoride [38]. Also, the development of such compounds as molecular catalysts for the activation and transformation of bound anionic substrates, and the development of selective anion transport systems for chemical or biological species are of prime interest. In view of the key role played by anions in chemistry and biology, the development of selective ligands for various anions opens many avenues in pure as well as applied research.

Experimental Part

General. All commercially available chemicals employed were reagent grade and used without further purification. Starting materials **4**, **7**, and **15** were obtained by described procedures (**4**, **7** [39]; **15**: by direct tosylation of 'tren' [40]) or by the reaction between *N*-tosylaziridine and NH_4OAc [41]. ^{1}H-NMR: *Bruker AC 200*; chemical shifts in ppm rel. to $SiMe_4$ (= 0 ppm) as internal standard. ^{13}C-NMR: broad-band decoupled. MS: fast-atom bombardment (FAB), positive-mode ZAB-HF were performed at the Laboratoire de Spectrométrie de Masse, Strasbourg. The microanalyses were made at the Service Central de Microanalyse du CNRS, Faculté de Chimie, Strasbourg.

pH-Metric Measurements. They were performed with a *Metrohm-636* titrimeter in a cell thermostated at 25 ± 0.1°, using stirred solns. under N_2. The log K_n values of the compounds were determined by titration of a soln. containing typically 10^{-3} M of the polyamine TsOH salt with 0.1N $(Me_4N)OH$ in the presence of 0.1M $(Me_4N)TsO$. The log K_s^n values of the complexes were determined by titration of a soln. containing 10^{-3} M of the polyamine TsOH salt and 0.015M of the Me_4N^+ salt of the desired halide with 0.1N $(Me_4N)OH$ in the presence of 0.1M $(Me_4N)TsO$. Data from all titrations were analyzed by the computer program SUPERQUAD [42].

N,N'-*(Ethane-1,2-diyl)bis[*N-*(cyanomethyl)-4-methylbenzenesulfonamide]* (**5**). A mixture of **4** (36.8 g, 0.1 mol), $ClCH_2CN$ (30.2 g, 0.4 mol), and K_2CO_3 (27.6 g, 0.2 mol) in 250 ml of DMF was stirred at r.t. for 5 days. More $ClCH_2CN$ (15.1 g, 0.2 mol) and K_2CO_3 (27.6 g, 0.2 mol) were added, and stirring was continued for 5 days. The mixture was poured into 2 l of H_2O, the precipitate filtered washed with H_2O, and dried, and the solid residue recrystallized from DMF/abs. EtOH: 34.8 g (78%). M.p. 204°. ^{1}H-NMR ($CDCl_3$): 2.46 (*s*, 2 Me); 3.42 (*s*, NCH_2CH_2N); 4.42 (*s*, 2 CH_2CN); 7.39, 7.74 (2*m*, 8 arom. H). Anal. calc. for $C_{20}H_{22}N_4O_4S_2$ (446.53): C 53.79, H 4.97, N 12.55; found: C 53.99, H 4.99, N 12.40.

N,N'-*(Ethane-1,2-diyl)bis[*N-*(2-aminoethyl)-4-methylbenzenesulfonamide]* (**6**). To a soln. of **5** (13.88 g, 0.031 mol) in 50 ml of anh. THF under N_2, 210 ml of 0.4M diborane in THF were added by syringe. The mixture was stirred and refluxed for 12 h. After cooling to r.t., dist. H_2O was added cautiously to decompose the excess of diborane. The solvent was evaporated, and the crude aminoborane derivative obtained was treated with 150 ml of 6N HCl at 90° for 3 h. The solvent was evaporated, and 200 ml 1N NaOH were added to the residue; this soln. was extracted with $CHCl_3$ (3 × 100 ml). The combined $CHCl_3$ extract was washed with H_2O, dried (Na_2SO_4), and evaporated and the residue dried *in vacuo*: **6** (13.7 g, 97%). Pale yellow viscous oil which was used for the next step without further purification. ^{1}H-NMR ($CDCl_3$): 2.40 (*s*, 2 Me); 2.86 (*t*, 2 $CH_2N(Ts)CH_2$); 3.12 (*t*, 2 H_2NCH_2); 3.28 (*s*, 2 $CH_2N(Ts)CH_2$); 7.30, 7.67 (2*m*, 8 arom. H).

4,7,13,16-Tetratosyl-1,4,7,10,13,16-hexaazacyclooctadecane-2,9-dione (**8**). For the macrocyclization step, the apparatus described in [6] was used. Two solns. in CH_2Cl_2/toluene 6:4 were prepared and transferred into two addition funnels; diamine **6** (13.7 g, 0.030 mol) and Et_3N (6.1 g, 0.060 mol) in 500 ml of solvent, and diacyl dichloride **7** (16.5 g, 0.0316 mol) in 500 ml of solvent. These solns. were simultaneously added dropwise within *ca.* 7 h to 1.5 l of CH_2Cl_2/toluene 6:4 under N_2 and vigorous stirring. After evaporation, the residue obtained was dissolved in CH_2Cl_2 (300 ml), the soln. washed with H_2O, dried (Na_2SO_4), and evaporated, and the residue chromatographed (silica gel, 1% MeOH/$CHCl_2$). Compound **8** was recrystallized from MeOH (10.8 g, 38%). M.p. 123–125°. ^{1}H-NMR ($CDCl_3$): 2.40, 2.43 (2br. *s*, 4 Me); 3.31, 3.41 (2br. *s*, 16 H, NCH_2CH_2NTs, $TsNCH_2CH_2NTs$); 3.81 (*s*, 4 H, $NCOCH_2NTs$); 6.75 (br. *s*, 2 HNCO); 7.30, 7.70 (2*m*, 16 arom. H). Anal. calc. for $C_{40}H_{50}N_6O_{10}S_4$ (903.09): C 53.13, H 5.58, N 9.31; found: C 53.14, H 5.54, N 8.85.

1,4,10,13-Tetratosyl-1,4,7,10,13,16-hexaazacyclooctadecane (**9**). As described for **6**, with **8** (10.3 g, 0.0115 mol), suspended in THF (50 ml), and 0.5M diborane in THF (200 ml; r.t. for 4 h and reflux for 20 h), then 6N HCl 100 ml; 80° for 2 h), 10% aq. NaOH soln. (100 ml), and CH_2Cl_2 (3 × 100 ml). Chromatography (alumina, 0.5% MeOH/CH_2Cl_2) and recrystallization from CH_2Cl_2/heptane gave 8.5 g (85%), of **9**. M.p. 213° ([27]: 208–212°). ^{1}H-NMR ($CDCl_3$): 1.6 (br., 2 NH); 2.44 (*s*, 4 Me); 2.80 (*t*, 8 H, $HNCH_2$); 3.19 (*t*, 8 H, $HNCH_2CH_2NTs$); 3.38 (*s*, 8 H, $TsNCH_2CH_2NTs$); 7.32, 7.70 (2*m*, 16 arom. H). ^{13}C-NMR ($CDCl_3$): 143.7, 134.8, 129.8, 127.5 (arom. C): 50.8, 49.7, 49.1 (NCH_2); 21.5 (Me). Anal. calc. for $C_{40}H_{54}N_6O_8S_4$ (875.12): C 54.89, H 6.22, N 9.60; found: C 54.64, H 6.05, N 9.42.

4,7,13,16,21,24-Hexatosyl-1,4,7,10,13,16,21,24-octaazabicyclo[8.8.8]hexacosane-2,9-dione (**10**). As described for **8** with solns. in CH_2Cl_2/toluene 8:2, *i.e.* **10** (8.5 g, 9.7 mmol) and Et_3N (2.02 g, 20 mmol) in 500 ml of solvent and **7** (5.21 g, 10 mmol) in 500 ml of solvent (addition *ca.* 8 h). Workup with CH_2Cl_2 (200 ml) and chromatography (silica gel, 0.5% MeOH/CH_2Cl_2 for **10** and 1% MeOH/CH_2Cl_2 for **12**) gave **10** which was recrystallized from CH_2Cl_2/toluene (3.55 g, 28%). M.p. 250°. ^{1}H-NMR ($CDCl_3$): 2.41–2.44 (3br. *s*, 6 Me); 2.6–3.7 (br. *m*, 28 H, NCH_2CH_2NTs, $TsNCH_2CH_2NTs$); 4.37 (br. *s*, 4 H, $NCOCH_2NTs$); 7.21–7.68 (*m*, 24 arom. H). MS: 1323 ([*M* + H]$^+$). Anal. calc. for $C_{60}H_{74}N_8O_{14}S_6$ (1323.62): C 54.44, H 5.64, N 8.47; found: C 54.59, H. 5.78, N 8.46.

Dimer **12** (2.35 g, 9%) was crystallized from $CH_2Cl_2/CHCl_3$. ^{1}H-NMR ($CDCl_3$): 2.32–2.43 (br., 36 H, Me); 2.60–4.60 (br. *m*, 64 H, NCH_2CH_2NTs, $TsNCH_2CH_2NTs$, $NCOCH_2NTs$); 7.10–7.90 (br. *m*, 48 arom. H). MS: 2648 ([*M* + H]$^+$). Anal. calc. for $C_{120}H_{148}N_{16}O_{28}S_{12}\cdot CHCl_3$ (2647.26): C 52.58, H 5.43, N 8.11; found: C 52.41, H 5.32, N 8.03.

4,7,13,16,21,24-Hexatosyl-1,4,7,10,13,16,21,24-octaazabicyclo[8.8.8]hexacosane (**11**). As described for **6**, with **10** (3 g, 2.26 mmol), suspended in THF (50 ml), and 0.5M diborane in THF (50 ml; reflux for 20 h), then 6N HCl (80° for 2 h), 10% aq. NaOH soln. (50 ml), and CH_2Cl_2 (3 × 100 ml). Chromatography (alumina, CH_2Cl_2) and recrystallization from CH_2Cl_2/toluene gave 2.65 g, (90%) of **11**. M.p. 178–180°. ^{1}H-NMR (CDCl): 2.43 (*s*, 18 H, Me); 2.68 (*t*, 12 H, NCH_2); 3.21 (*t*, 12 H, NCH_2CH_2NTs); 3.28 (*s*, 12 H, $TsNCH_2CH_2NTs$); 7.30, 7.67 (2*m*, 24 arom. H). ^{13}C-NMR ($CDCl_3$): 143.7, 135.9, 129.9, 127.4 (arom. C); 55.9, 49.2, 48.9 (NCH_2); 21.5 (Me). Anal. calc. for $C_{60}H_{78}N_8O_{12}S_6\cdot 0.5$ toluene (1295.68): C 56.84, H 6.16, N 8.35; found: C 56.47, H 6.20, N 8.06.

1,4,7,10,13,16,21,24-Octaazabicyclo[8.8.8]hexacosane (**1**). A mixture of **11** (2.1 g, 1.6 mmol), phenol (5 g, 5.3 mmol), and 100 ml of 33% HBr in AcOH was heated at 80° for 16 h. The soln.was cooled, the acids were removed under vacuum, and 100 ml of toluene were added and evaporated to remove the rest of AcOH. The residue was taken up in 100 ml of CH_2Cl and 50 ml of H_2O, and the aq. layer was washed with CH_2Cl_2 (3 ×) and concentrated to 5 ml. This soln. was passed over *Dowex 1* × *8* resin (basic form) and then evaporated to give **1** (510 mg, 86%) as a white powder which was transformed immediately in its hydrochloride: an aq. soln. of the free amine was acidified with conc. HCl soln. and evaporated. The residue was crystallized in EtOH: **1**·6 HCl. M.p. > 250°. ^{13}C-NMR (D_2O): 53.7, 49.1, 47.1 (NCH_2). Anal. calc. for $C_{18}H_{54}Cl_6N_8O_3$ (643.41): C 33.60, H 8.46, N 17.42; found: C 34.02, H 8.76, N 17.37.

Compound **1** has also been obtained by the condensation method described by *Nelson* and coworkers [24][1]): yield 25%. M.p. 116°. ^{1}H-NMR (500 MHz, $CDCl_3$): 2.50 (*t*, 12 H, NCH_2); 2.74 (*t*, 12 H, NCH_2CH_2NH); 2.77 (*s*, 12 H, $NHCH_2CH_2NH$). MS: 371 ([*M* + H]$^+$). Anal. calc. for $C_{18}H_{42}N_8$ (370.59): C 58.34, H 11.42, N 30.24; found: C 58.22, H. 11.37, N 30.04.

For the pH-metric measurements, the salt **1**·8 TsOH was prepared by treatment of the free amine **1** with an excess of TsOH. The salt **1**·8 TsOH was crystallized from MeOH/Et_2O. ^{1}H-NMR (D_2O): 2.56 (*s*, 24 H, Me); 2.89 (br. *t*, 12 H, NCH_2); 3.25 (br. *t*, 12 H, NCH_2CH_2NH); 3.48 (*s*, 12 H, $NHCH_2CH_2NH$); 7.54, 7.86 (*m*, 32 arom. H). Anal. calc. for $C_{74}H_{106}N_8O_{24}S_8\cdot 4\,H_2O$ (1748.16): C 48.84, H 6.27, N 6.16; found: C 48.43, H 6.17, N 6.50.

4,7,13,16,21,24-Hexamethyl-1,4,7,10,13,16,21,24-octaazabicyclo[8.8.8]hexacosane (**2**). To a soln. of the free

---

[1]) We thank *Tim Lange* for his contribution in the synthesis of **1**.

amine **1** (250 mg, 0.67 mmol) in 90% formic acid (50 ml), a large excess of paraformaldehyde (12.5 g) was added. The mixture was heated under vigorous stirring. After complete dissolution, the soln. was refluxed for 3 days under Ar(turned orange) and then evaporated. H_2O (50 ml) was added to the residue, the soln. basified to pH 10 by addition of KOH and extracted with $CHCl_3$ (3 × 150 ml), the extract evaporated, and the obtained yellow oil dissolved with an aq. soln. containing TsOH (2 g, 10 mmol). The solvent was evaporated the yellowish solid dissolved in MeOH, Et_2O added, and the precipitate filtered and washed with Et_2O: **2**·6 TsOH (611 mg, 58%). The salt was recrystallized from MeOH/EtOH/Et_2O. ^{1}H-NMR (D_2O): 2.58 (*s*, 18 H, *Me*C_6H_4); 2.90 (*s*, 18 H, MeN); 3.34 (br. *m*, 24 H, NCH_2CH_2NMe); 3.48 (*s*, 12 H, MeNCH_2CH_2NMe); 7.56, 7.88 (24 arom. H). ^{13}C-NMR (D_2O): 144.4, 141.3, 131.4, 127.2 (arom. C); 55.5, 51.9, 51.5, 43.5 (CH_2, Me); 22.4 (*Me*C_6H_4). MS (free **2**): 455.5 ([*M* + H]$^+$). Anal. calc. for $C_{24}H_{54}N_8$·6 TsOH·4 H_2O (1487.94): C 50.83, H 7.06, N 7.19; found: C 50.45, H 7.05, N 7.47.

N,N′,N″-*[Nitrilo(ethane-2,1-diyl)]tris*{N-*[2-(methoxycarbonyl)ethyl]-4-methylbenzenesulfonamide*} (**16**). A mixture of **15** (20 g, 0.0329 mol), methyl acrylate (15 ml, 0.166 mol), and K_2CO_3 (30 g) in MeCN (300 ml) was stirred at r.t. for 12 h. After evaporation, the residue was taken up with CH_2Cl_2 (200 ml) and H_2O (100 ml), the org. layer washed with H_2O, dried (SO_4Na_2), and evaporated, and the brownish oil chromatographed (alumina (200 g), CH_2Cl_2): pure **16** (25.7 g, 90%). Thick viscous oil. ^{1}H-NMR ($CDCl_3$): 2.41 (*s*, 3 Me); 2.62, 2.71 (2*t*, 12 H, CH_2NTsCH_2); 3.16 (*t*, 6 H, CH_2N); 3.41 (*t*, 6 H, CH_2CO); 3.64 (*s*, 3 COOMe); 7.30, 7.71 (*m*, 12 arom. H). MS: 867.2 ([*M* + H]$^+$). Anal. calc. for $C_{39}H_{54}N_4O_{12}S_3$ (867.04): C 54.02, H 6.28, N 6.46; found: C 54.19, H 6.52, N 6.60.

N,N′,N″-*[Nitrilo(ethane-2,1-diyl)]tris[*N-*(3-hydroxypropyl)-4-methylbenzenesulfonamide]* (**17**). A soln. of **16** (25 g, 0.029 mol) in dry THF (200 ml) was added dropwise to a stirred suspension of $LiAlH_4$ (12 g, 0.32 mol) in dry THF (200 ml) at 0° within 30 min. The mixture was allowed to reach r.t. stirred for a further 24 h, and then cooled in a dry ice/acetone bath. Sat. Na_2SO_4 soln. (*ca.* 60 ml) was added cautiously until the ensuing effervescence abated. The mixture was filtered through *Celite*, the solid washed with copious amounts of CH_2Cl_2, the combined soln. evaporated, and the oil chromatographed (silica gel (300 g), 2% MeOH/CH_2Cl_2): **17** (18.8 g, 83%). Oil. ^{1}H-NMR ($CDCl_3$): 1.77 (*m*, 9 H, $CH_2CH_2CH_2$, CH_2OH); 2.42 (*s*, 3 Me); 2.78 (*t*, 6 H, CH_2N); 3.15, 3.23 (2*t*, 12 H, CH_2NTs); 3.69 (*t*, 6 H, CH_2OH); 7.30, 7.70 (*m*, 12 arom. H). MS: 783.2 ([*M* + H]$^+$). Anal. calc. for $C_{36}H_{54}S_3O_9N_4$ (783.0): C 55.21, H 6.95, N 7.16; found: C 54.75, H 6.91, N 6.90.

N,N′,N″-*[Nitrilo(ethane-2,1-diyl)]tris*{N-*[3-(methylsulfonyloxy)propyl]-4-methylbenzenesulfonamide*} (**18**). Et_3N (18 ml, 0.13 mol) was added to a soln. of **17** (13 g, 0.0166 mol) in 200 ml of dry CH_2Cl_2 (freshly distilled over CaH_2). The soln. was cooled to 0°, and MsCl (4 ml, 0.052 mol) in dry CH_2Cl_2 (20 ml) was added dropwise in 20 min. The mixture was allowed to reach r.t., and stirring was continued for 12 h. The soln. was washed rapidly with cooled H_2O (100 ml), cooled 1N HCl, sat. $NaHCO_3$ soln. (100 ml), and H_2O (100 ml) and then dried (Na_2SO_4). Evaporation gave **18** (16.5 g, 98%). Due to its unstability, **18** was used directly for the cyclization step. ^{1}H-NMR ($CDCl_3$): 1.98–2.08 (*m*, 6 H, $CH_2CH_2CH_2$); 2.42 (*s*, 3 *Me*C_6H_4); 2.77 (*m*, 6 H, CH_2N); 3.00 (*s*, 3 Ms); 3.12–3.24 (*m*, 12 H, CH_2NTsCH_2); 4.28 (*t*, 6 H, CH_2OMs); 7.32, 7.69 (*m*, 12 arom. H).

4,8,14,18,23,27-Hexatosyl-1,4,8,11,14,18,23,27-octaazabicyclo[9.9.9]nonacosane (**19**). A mixture of **15** (9.85 g, 0.0162 mol), Cs_2CO_3 (40 g, 0.123 mol), and DMF (400 ml) was heated under Ar to 90°. To this stirred mixture, **18** (16.5 g, 0.0162 mol) in DMF (150 ml) was added dropwise within 6 h. Heating was continued for 48 h. After cooling, the mixture was filtered, the solid residue washed with CH_2Cl_2, the filtrate evaporated, the residue treated with CH_2Cl_2 (300 ml) and 1N NaOH (100 ml), and the org. layer washed with H_2O, dried (SO_4Na_2), and evaporated. Chromatography (alumina (300 g), 8% acetone/toluene) afforded pure **19** (6.85 g, 31%) which was crystallized from CH_2Cl_2/toluene/heptane. M.p. 158°. ^{1}H-NMR ($CDCl_3$): 1.90 (*m*, 6 H, $CH_2CH_2CH_2$); 2.42 (*s*, 6 Me); 2.90 (*m*, 12 H, CH_2N); 3.09 (*m*, 24 H, CH_2NTs); 7.32, 7.68 (*m*, 24 arom. H). ^{13}C-NMR ($CDCl_3$): 143.6, 135.1, 130.0, 127.3 (arom. C); 54.1 (CH_2N); 49.0, 47.6 (CH_2NTs); 29.8 ($CH_2CH_2CH_2$); 21.5 (Me). MS: 1337.4 ([*M* + H]$^+$). Anal. calc. for $C_{63}H_{84}N_8O_{12}S_6$ (1337.74): C 56.56, H 6.32, N 8.37; found: C 56.66, H 6.12, N 8.38.

1,4,8,11,14,18,23,27-Octaazabicyclo[9.9.9]nonacosane (**3**). A mixture of **19** (2 g, 1.49 mmol), phenol (4 g, 21 mmol), and 75 ml of 33% HBr in AcOH was heated at 90° for 16 h under a well ventilated hood. After cooling, the precipitate was filtered and washed with Et_2O. The crude HBr salt was dissolved in H_2O and passed over a *Dowex 1 × 8* resin (basic form). The free amine soln. was treated with an excess of conc. HCl soln. After evaporation, crystallization from EtOH gave **3**·6 HCl (850 mg, 85%). M.p. > 250°. ^{1}H-NMR (D_2O): 2.55 (*m*, 6 H, $CH_2CH_2CH_2$); 3.09 (br. *t*, 12 H, CH_2N); 3.57, 3.60 (br. *m*, 24 H, CH_2NHCH_2). Anal. calc. for $C_{21}H_{54}Cl_6N_8$·2 H_2O (631.41): C 37.78, H 8.75, N 16.79; found: C 37.71, H 9.04, N 16.26.

For the pH-metric measurements and X-ray diffraction studies, the salt **3**·6 TsOH was prepared by treatment of the free amine **3** with 7 equiv. of TsOH and crystallization from EtOH. ^{1}H-NMR (D_2O): 2.25 (br. *m*, 6 H, $CH_2CH_2CH_2$); 2.51 (*s*, 6 *Me*C_6H_4); 3.05, 3.36 (br. *t*, br. *m*, 36 H, CH_2N); 7.50, 7.81 (*m*, 24 arom. H). ^{13}C-NMR (D_2O): 144.8, 141.3, 131.6, 127.3 (arom. C); 50.7, 45.6, 44.8 (CH_2N); 23.2 ($CH_2CH_2CH_2$); 22.5 (*Me*C_6H_4). Anal. calc. for $C_{63}H_{96}N_8O_{18}S_6$·2 H_2O (1481.84): C 51.06, H 6.80, N 7.56; found: C 50.84, H 6.79, N 7.84.

4,7,13,16,22,25,31,34,39,42,47,50-Dodecatosyl-1,4,7,10,13,16,19,22,25,28,31,34,39,42,47,50-hexadecaazatricyclo[26.8.8.8^{10,19}]dodecapentacontane (**13**). As described for **6**, with **12** (500 mg, 0.19 mmol) suspended in THF (25 ml), and 1M diborane in THF (20 ml; 15 h reflux), then 6N HCl (50 ml; 80° for 20 h), 5% aq. NaOH soln. (100 ml), and $CHCl_3$ (100 ml): 472 mg (96%) of **13**. ^{1}H-NMR ($CDCl_3$): 2.38 (36 H, Me); 2.75 (br., 24 H, NCH_2CH_2NTs); 3.12 (*s*, 16 H, $NTsCH_2CH_2NTs$); 3.22 (br., 24 H, NCH_2CH_2NTs); 3.30 (*s*, 8 H, $NTsCH_{2CH_2}NTs$); 7.21, 7.25, 7.28, 7.32, 7.62, 7.66, 7.71, 7.75 (4*d*, 48 arom. H). ^{13}C-NMR ($CDCl_3$): 143.5, 136.2, 135.8, 129.9, 127.5, 127.4 (arom. C); 54.1, 52.9, 49.8, 48.8, 48.4, 48.1 (CH_2); 21.6 (Me). MS: 2592 ([M + H]$^+$), 2437 ([M – Ts]$^+$), 2281 ([M – 2 Ts]$^+$), 2125 ([M – 3 Ts]$^+$),1969 ([M – 4Ts]$^+$), 1296 ([M + H]$^{++}$). Anal. calc. for $C_{120}H_{156}N_{16}O_{24}S_{12}$ (2591.38): C 55.62, H 6.07, N 8.65; found: C 55.44, H 6.24, N 8.53.

1,4,7,10,13,16,19,22,25,28,31,34,39,42,47,50-Hexadecaazatricyclo[26.8.8.8^{10,19}]dodecapentacontane (**14**). The mixture of **13** (336 mg, 0.13 mmol), phenol (300 mg, large excess), and 100 ml of 33% HBr in AcOH was heated at 80° for 2 days. After the soln. was cooled, the acids were evaporated. The residue was taken up in 100 ml of CH_2Cl_2 and 50 ml of 1N HCl, and the aq. layer was washed twice with CH_2Cl_2 and evaporated: 272 mg of HBr salt of **14**. ^{1}H-NMR (D_2O): 3.19 (br., 24 H, $NHCH_2CH_2NH$); 3.61 (br., 24 H, NCH_2CH_2NH); 3.86 (*s*, 8 H, $NHCH_2CH_2NH$); 3.91 (*s*, 16 H, $NHCH_2CH_2NH$). ^{13}C-NMR (D_2O): 52.5 49.3, 48.2, 47.1, 46.1, 45.7 (CH_2). MS: 741 ([M + H]$^+$), 822 ([M + HBr]$^+$), 903 ([M + 2 HBr]$^+$), 984 ([M + 3 HBr]$^+$).

Tosylate Salt of **14**. The HBr salt of **14** was dissolved in 10 ml H_2O and passed over a *Dowex 1 × 8* resin (basic form). The soln. was evaporated and then acidified with a soln. of TsOH (500 mg, excess) in H_2O. The mixture was evaporated, the residue dissolved in MeOH, and the soln. treated with Et_2O. After triturating for 3 days, the solid was filtered off under vacuum to yield a very sticky hygroscopic white solid which was redissolved in abs. EtOH. The soln. was evaporated under reduced pressure: 80 mg of **14**·12 TsOH. ^{1}H-NMR (D_2O): 2.55 (*s*, 36 H, Me); 2.94 (br., 16 H, NCH_2CH_2NH); 3.09 (br., 8 H, NCH_2CH_2NH); 3.19 (br., 16 H, NCH_2CH_2NH); 3.38 (*s*, 16 H, $NHCH_2CH_2NH$); 3.52 (br., 8 H, NCH_2CH_2NH); 3.72 (*s*, 8 H, $NHCH_2CH_2NH$); 7.51, 7.55, 7.84, 7.88 (2*d*, 48 H, Ts). Anal. calc. for $C_{120}H_{180}N_{16}O_{36}S_{12}\cdot 4\ H_2O$ (2879.62): C 50.05, H 6.58, N 7.80; found: C 49.94, H 6.57, N 7.65.

Crystal-Structure Analysis. The crystallographic data of the three structures are summarized in *Table 3*. All diffraction data were recorded on a *Philips-PW1100* automatic diffractometer. The intensities were corrected for *Lorentz*-polarization but not for absorption. The structures were solved by direct methods [43] and refined by large blocks least squares method [44]. H-Atoms were located to their theoretical position at 1.0 Å of the atoms to which they were bonded, and assigned the equivalent isotropic thermal factor of the bonded C- or N-atom.

*Fluoride Cryptate [$F^-\subset$ **1**·6 H^+].* Aside from the included F^-, two other F^- ions are found outside the cavity along with a Cl^- and two PF_6^- ions. One of the latter is very disordered around one F–P–F axis (four positions were located, corresponding to occupancy factors of 45, 20, 20, and 15%). In addition, the asymmetric unit contains 5 H_2O molecules (one being in two exclusive positions), contributing to a very complicated H-network.

Uncomplexed Macrobicycle **3**·6 H^+. Of the six tosylate counterions, one is completely disordered between two sites (occupation factor: 75 and 25%). The three O-atoms of another one are exchanging between two 50% occupied orientations. Three H_2O molecules, out of 8, occupy non-stoichiometric sites.

Chloride Cryptate [$Cl^-\subset$ **3**·6 H^+]. With the included Cl^-, 5 other anions and five H_2O molecules (three of them non-stoichiometric) belong to the asymmetric unit. The observed minimum and maximum density peaks in the difference *Fourier* map are –0.6 and +0.5 eA^{-3}.

REFERENCES

[1] J. L. Pierre, P. Baret, *Bull. Soc. Chim. Fr.* **1983,** 367.
[2] B. Dietrich, in 'Inclusion Compounds'; Eds. J. L. Atwood, J. E. D. Davies, and D. D. MacNicol, Academic Press, London, 1984, Vol. 2, pp. 337–405.
[3] E. Kimura, *Topics Curr. Chem.* **1985,** *128,* 113.
[4] F. P. Schmidtchen, *Nachr. Chem. Tech. Lab.* **1988,** *36,* 8.
[5] A. Bianchi, M. Micheloni, P. Paoletti, *Pure Appl. Chem.* **1988,** *60,* 525.
[6] L. F. Lindoy, 'The Chemistry of Macrocyclic Ligand Complexes', Cambridge University Press, Cambridge, U.K., 1989.
[7] F. P. Schmidtchen, A. Gleich, A. Schummer, *Pure Appl. Chem.* **1989,** *61,* 1535.
[8] R. M. Izatt, K. Pawlak, J. S. Bradshaw, R. L. Bruening, *Chem. Rev.* **1991,** *91,* 1721.
[9] B. Dietrich, *Pure Appl. Chem.* **1993,** *65,* 1457.

[10] J.L. Sessler, M. Cyr, H. Furuta, V. Kral, T. Mooy, T. Morishima, M. Shionoya, S. Weghorn, *Pure Appl. Chem.* **1993,** *65,* 393.
[11] J.-M. Lehn, 'Supramolecular Chemistry', VCH, Weinheim, 1995, Chapt. 3.
[12] C. Seel, A. Galan, J. de Mendoza, *Topics Curr. Chem.* **1995,** *175,* 101.
[13] H.E. Simmons, C.H. Park, *J. Am. Chem. Soc.* **1968,** *90,* 2428; C.H. Park, H.E. Simmons, *ibid.* **1968,** *90,* 2431; R.A. Bell, G.G. Christoph, F.P. Fronczek, R.E. Marsh, *Science* **1975,** *190,* 151.
[14] E. Graf, J.-M. Lehn, *J. Am. Chem. Soc.* **1976,** *98,* 6403.
[15] J.-P. Kintzinger, J.-M. Lehn, E. Kauffmann, J.L. Dye, A.I. Popov, *J. Am. Chem. Soc.* **1983,** *105,* 7549.
[16] B. Metz, J.M. Rosalsky, R. Weiss, *J. Chem. Soc., Chem. Commun.* **1976,** 533.
[17] F.P. Schmidtchen, *Angew. Chem. Int. Ed.* **1977,** *16,* 720; F.P. Schmidtchen, G. Müller, *J. Chem. Soc., Chem. Commun.* **1984,** 1115; F.P. Schmidtchen, *Chem. Ber.* **1981,** *114,* 597; K. Worm, F.P. Schmidtchen, A. Schier, A. Schäfer, M. Hesse, *Angew. Chem. Int. Ed.* **1994,** *33,* 327; K. Worm, F.P. Schmidtchen, *ibid.* **1995,** *34,* 65.
[18] J.-M. Lehn, E. Sonveaux, A.K. Willard, *J. Am. Chem. Soc.* **1978,** *100,* 4914.
[19] B. Dietrich, J. Guilhelm, J.-M. Lehn, C. Pascard, E. Sonveaux, *Helv. Chim. Acta* **1984,** *67,* 91.
[20] D. Heyer, J.-M. Lehn, *Tetrahedron Lett.* **1986,** *27,* 5869.
[21] M.W. Hosseini, J.-M. Lehn, *Helv. Chim. Acta* **1988,** *71,* 749.
[22] B. Dietrich, J.-M. Lehn, J. Guilhem, C. Pascard, *Tetrahedron Lett.* **1989,** *30,* 4125.
[23] J.-M. Lehn, *Structure Bonding* **1973,** *16,* 1.
[24] J. Hunter, J. Nelson, C. Harding, McCann, V. McKee, *J. Chem. Soc., Chem. Commun.* **1990,** 1148.
[25] J.-M. Lehn, F. Montavon, *Helv. Chim. Acta* **1978,** *61,* 67.
[26] N. Martin, V. McKee, J. Nelson, *Inorg. Chim. Acta* **1994,** *218,* 5.
[27] M. Takada, K. Saigo, T. Hirai, I. Ohchi, M. Tajima, M. Seno, M. Hasegawa, *Bull. Chem. Soc. Jpn.* **1988,** *61,* 2413.
[28] J. Cheney, J.-P. Kintzinger, J.-M. Lehn, *Nouv. J. Chim.* **1978,** *2,* 411.
[29] P.J. Hammond, P.D. Beer, C.D. Hall, *J. Chem. Soc., Chem. Commun.* **1983,** 1161.
[30] E. Chapoteau, B. Czech, A. Kumar, A. Pose, *J. Incl. Phenom.* **1988,** *6,* 41.
[31] T. Kumagai, S. Akabori, *Bull. Chem. Soc. Jpn.* **1989,** *62,* 3021.
[32] S.D. Reilly, G.R.K. Khalsa, D.K. Ford, J.R. Brainard, B.P. Hay, P.H. Smith, *Inorg. Chem.* **1995,** *34,* 569.
[33] M. Micheloni, A. Sabatini, P. Paoletti, *J. Chem. Soc., Perkin Trans. 2* **1978,** 828; V.J. Thöm, G.D. Hosken, R.D. Hancock, *Inorg. Chem.* **1985,** *24,* 3378; L.H. Tan, M.R. Taylor, K.P. Wainwright, P.A. Duckworth, *J. Chem. Soc., Dalton Trans.* **1993,** 2921.
[34] J.-M. Lehn, J.-P. Sauvage, *J. Am. Chem. Soc.* **1975,** *97,* 6700.
[35] J.L. Sessler, M.J. Cyr, V. Lynch, E. McGhee, J.A. Ibers, *J. Am. Chem. Soc.* **1990,** *112,* 2810.
[36] M. Shionoya, H. Furuta, V. Lynch, A. Harriman, J.L. Sessler, *J. Am. Chem. Soc.* **1992,** *114,* 5714.
[37] J.L. Sessler, M. Cyr, H. Furuta, V. Kral, T. Mooy, T. Morishima, M. Shionoya, S. Weghorn, *Pure Appl. Chem.* **1993,** *65,* 393.
[38] J.-M. Lehn, J.-P. Souchez, work in progress.
[39] H. Stetter, E. Roos, *Chem. Ber.* **1954,** *87,* 566; H. Stetter, K. Mayer, *ibid.* **1961,** *94,* 1410.
[40] R.H. Mizzoni, M.A. Hennessey, C.R. Scholz, *J. Am. Chem. Soc.* **1954,** *76,* 2414.
[41] B. Dietrich, M.W. Hosseini, J.-M. Lehn, R.B. Sessions, *Helv. Chim. Acta* **1985,** *68,* 289.
[42] P. Gans, A. Sabatini, A. Vacca, *J. Chem. Soc., Dalton Trans.* **1985,** 1195.
[43] G.M. Sheldrick, 'SHELXS86, Program for Crystal Structure Solution', University of Göttingen, Germany, 1986.
[44] G.M. Sheldrick, 'SHELX76, Program for Crystal Structure Determination', University of Cambridge, England, 1976.